HKIE THE HONG KONG INSTITUTION OF ENGINEERS 香港工程師學會

Axial capacity of open-ended steel pipe piles in sand: comparison of analytical methods and FEM modelling

Harry Ho Kan Lee[1] and Jun Yang[2]
[1] AECOM Asia Company Limited, Hong Kong, People's Republic of China
[2] Department of Civil Engineering, The University of Hong Kong, Hong Kong, People's Republic of China

ABSTRACT

This study investigates the axial capacity of open-ended steel pipe piles in sand through a combined analytical and numerical approach. A database of 26 field load tests from global offshore and nearshore projects was established to evaluate five design methods: API (2007), GEO (2006), ICP-05, UWA-05, and HKU-12. Comparative analyses show that CPT-based methods significantly outperform traditional technical standards, with lower prediction scatter and improved consistency in estimating total, base, and shaft capacities. Among these, HKU-12 achieved the closest agreement with measured capacities, followed by UWA-05, while API and GEO exhibited large variances due to limited consideration of soil plugging and simplified stress correlations. To complement the analytical evaluation, 3D FEM models were developed in PLAXIS to simulate installation-induced deformation and soil plugging. The simulations reproduced realistic load–settlement responses and showed that axial capacity is highly sensitive to the prescribed installation displacements. Best-fit results required much smaller displacement inputs than those suggested in an earlier study, indicating that installation effects for open-ended piles differ fundamentally from other displacement piles. Overall, the study demonstrates the accuracy of refined CPT-based methods and presents the potential of FEM modelling in improving the reliability of offshore pile design.

KEYWORDS Steel pipe piles; offshore pile construction; soil plugging, finite element method (FEM); geotechnical analysis; pile axial capacity

CONTACT Harry Ho Kan Lee harry.lee@aecom.com
Received 13 March 2026

1. Introduction

Open-ended steel pipe piles have become increasingly common with the growth of offshore infrastructure such as wind farms, cross-sea bridges, and oil and gas facilities, including the Hangzhou Bay Bridge, the Hong Kong–Zhuhai–Macao Bridge, and the Hong Kong Offshore LNG Terminal Project (Shea et al., 2022). This expansion has driven a rising demand for efficient piling systems. These piles offer key advantages in offshore environments: they penetrate soft and loose soils more easily than traditional piles and, due to their large diameters, can achieve high axial capacities with fewer piles, reducing construction time and complexity.

Current design standards take simplified approaches. API (2007) provides design factors based on the relative density of sand to estimate base and shaft resistance, while GEO (2006) applies constant reductions of 0.8 for base resistance and 0.5 for shaft resistance relative to closed-ended piles. These empirical factors may not fully reflect soil–pile interaction, leading to potential inaccuracies.

Extensive research has refined pile capacity predictions using Cone Penetration Test (CPT) data. Notable CPT-based methods include those developed by Imperial College London (Jardine et al., 2005), the University of Western Australia (Lehane et al., 2005a, 2005b), and the University of Hong Kong (Yu & Yang, 2012a, 2012b). Finite element modelling has also been used to study axial capacity. For example, Ko et al. (2015) modelled instrumented piles using ABAQUS, with diameters from 508 to 914.4 *mm* and lengths from 8.6 to 15.0 *m*.

This study compiles a database of 26 open-ended steel pipe piles to assess the accuracy of analytical methods including API, GEO, ICP-05, UWA-05, and HKU-12. Additionally, three piles were modelled using PLAXIS 3D (Version 20) to evaluate the suitability of finite element analysis for predicting axial capacity.

2. Soil plugging

Unlike other displacement piles, the axial capacity of open-ended steel pipe piles is influenced by soil entering their hollow sections. During installation, soil intrudes into the pile and mobilises inner shaft resistance until it equals the internal base resistance, forming a soil plug. This plug contributes significant resistance, allowing long open-ended piles to achieve capacities comparable to closed-ended piles (Lehane & Randolph, 2002).

Without soil plugging, a fully coring pile contains soil along its full length, and axial bearing capacity is comprised of inner shaft resistance τ_{in}, outer shaft resistance τ_{out}, and base friction of annulus $q_{annulus}$. Meanwhile, in a fully plugged pile, inner shaft resistance is replaced by a higher plug capacity q_{plug}. In practice, most piles exhibit partial plugging, where plug height lies between pile top and founding level.

The degree of plugging is commonly described by reference to Plug Length Ratio (PLR) and Incremental Filling Ratio (IFR), which relate to Pile Length L and Plug Height H. These were proposed by Paikowsky et al. (1989) and Paik and Lee (1993). Definitions of PLR and IFR and typical plugging scenarios are illustrated in Figure 1.

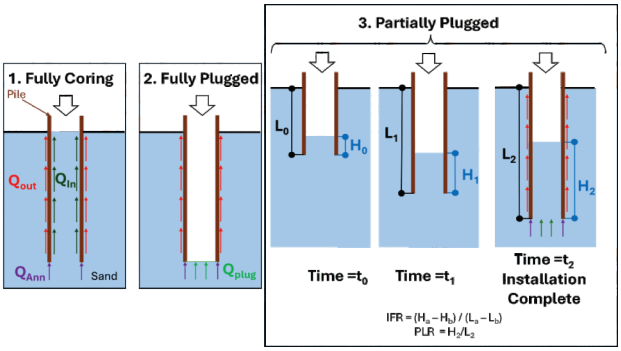

Figure 1. Soil plugging scenarios and physical meanings of IFR and PLR.

Estimations of IFR and PLR and their correlations have been proposed in various scientific papers, as presented below.

$$IFR_{average} = \min[1,(d/1.5)^{0.2}] \text{ by Lehane et al. (2005), (1)}$$

$$PLR = \min[1,(d)^{0.15}] \leq 1 \text{ by Yu and Yang (2012a), (2)}$$

$$PLR = 0.917IFR + 0.202 \text{ by Paik and Salgado (2003). (3)}$$

*where d = inner pile diameter in *m* and
IFRaverage = average IFR over 20 times the pile diameter of pile penetration.

3. Selected Analytical Methods

This study evaluates five analytical approaches commonly used to estimate the axial capacity of open-ended steel pipe piles in sand: API (2007), GEO (2006), ICP-05, UWA-05, and HKU-12. These methods differ significantly in their theoretical foundations, treatment of soil plugging, and use of in-situ test data, leading to variable predictive performance. The axial capacity is defined as the capacity when pile settlement is 10% of the outer pile diameter D. When determining base friction, CPT-based methods considered the influence zone to take appropriate average values.

3.1. Technical standards – API and GEO

Both technical standards from API (2007) and GEO (2006) are based on plasticity theories in accordance with the equations below:

$$q_b = \sigma'_v N_q \,\&\, \tau_z = \sigma'_v \beta. \quad (4)$$

where q_b is the unit base friction, σ'_v is effective overburden pressure, N_q is the bearing capacity factor, τ_z is the shaft friction at depth z, and β is the shaft resistance coefficient.

Under Section 6.4.3 of API, N_q can be correlated based on soil classification using relative density D_r. β relates to the soil–pile friction angle with a 0.8 factor as the coefficient of lateral earth pressure.

For the GEO method, N_q is correlated with angle of shear resistance per GEO Publication No. 1/2006 (GEO, 2006). Typical values of β and correlations with angle of shear resistance are given therein. Reduction factors of 0.8 and 0.5 on base resistance and shaft resistance, respectively, are applied to the obtained values for open-ended steel pipe piles, as specified in Section 6.4.4.8 (GEO, 2006).

3.2. Imperial College Method (ICP-05)

ICP-05 is an empirical CPT-based method published in 2005 by Jardine et al., developed using 11 pile test datasets. It concerns whether a rigid basal plug is formed during static loading by relating to the inner pile diameter d, relative density D_r, and cone tip resistance q_c. For piles classified as not fully coring, the plugging-adjusted base resistance equation is applied. Shaft resistance is derived from Coulomb Criterion relating shear stress to normal stress such that local radial stress σ'_r and modified radius R* for the effect of wall thickness and soil plugging of open-ended piles are determined. Increase of radial stress $\Delta\sigma_r'$ and corresponding change of radial displacement Δr due to observed dilation, were also incorporated. ICP-05 adopts the arithmetic mean at 1.5D above and below the pile tip to estimate average cone tip resistance $q_{c,a}$.

3.3. University of Western Australia Method (UWA-05)

The UWA-05 method, proposed by Lehane (2005a, 2005b), is a refinement of the ICP-05 method, based on 13 test data subjects. It adjusted some assumptions of ICP-05 and considered the extent of plugging. To represent partial plugging, Lehane et al. (2005a) proposed using the average IFR ($IFR_{average}$) over the last 3D of penetration depth, known as the Final Filling Ratio (FFR). If FFR data are unavailable, PLR or $IFR_{average}$ can be taken. A maximum soil–pile interface friction angle (δ_{cv}) of 29° is adopted to consider changes in soil roughness during installation.

The effect of pile size on sand displacement during installation is considered by introducing Base Effective Area Ratio (A_{rb}*) and Shaft Effective Area Ratio (A_{rs}) to relate diameter, wall thickness, and plug extent.

Lower bound and upper bound values of 0.15 and 0.6 for unit base resistance q_b were introduced by Lehane et al. (2005a). The upper bond matches the original assumption of ICP-05.

Improvements to the shaft resistance formulation include a revised dependence on relative depth h/D and the assumption that local radial stress is independent of effective overburden pressure.

In the determination of the influence zone for $q_{c,a}$, UWA-05 made use of the Dutch Method such that $q_{c,a}$ is an average of two parameters: average cone tip resistance of the CPT envelope and minimum envelope within 0.7D to 4D below the pile tip, and that of the minimum envelope at 8D above the pile tip.

3.4. The University of Hong Kong Method (HKU-12)

The HKU method is a CPT-based design method advanced from ICP-05 and UWA-05 by Yu and Yang (2012a, 2012b) on plugging and interface behaviours. The method replaces IFR with a more practical PLR, which only requires one measurement of plug length after pile installation. It also includes the slenderness ratio L/D to reflect partial embedment conditions and divides base capacity into annulus capacity and plug capacity to allow separate analyses.

For shaft resistance, HKU-12 introduces a soil-squeezing parameter ρ and a modified diameter D* to capture reductions in radial stress due to internal plugging. A soil squeezing ratio was introduced to compare the volume of squeezed soil and corresponding pile for developing relationships between squeezed soil volume, plug length, reduction in radial effective stress, and shaft friction. Yu and Yang (2012b) suggested a reduction via modified diameter in estimating the increase of radial stress through a cavity expansion model.

In the determination of the influence zone for $q_{c,a}$, HKU-12 adopted the approach proposed by Yang (2006), which incorporates sand compressibility when defining the depth ranges used. For low-compressibility sand, the influence zones above the pile tip (A) and below the pile tip (B) are 1.5D-2.5D and 3.5D-5.5D, respectively. For high-compressibility sand, influence zones above the pile tip (A) and below the pile tip (B) are 0.5D-1.5D and 1.5D-3D.

The geometric mean of cone tip resistances above tip M_A and below tip M_B can be calculated, respectively, as:

$$M_A \; OR \; M_B = \sqrt[n]{q_{c,1} * q_{c,2} * q_{c,3} \cdots q_{c,n}}. \qquad (5)$$

such that $q_{c,a}$ would be the average of M_A and M_B if M_B is greater than or equal to M_A. Otherwise, $q_{c,a}$ is equal to M_A.

Equations adopted by the mentioned analytical methods from technical standards and studies are summarised in Table 1.

Table 1. Equations of selected analytical methods for axial capacity.

Methods	Equations for Base Capacity	Equations for Shaft Capacity
API	$q_b = \sigma'_v N_q$	$\tau_z = \sigma'_v \beta$
GEO	$q_b = \sigma'_v N_q * 0.8$	$\tau_z = \sigma'_v \beta * 0.5$
ICP-05	$d < 0.02 * (D_r - 30)$ $\frac{d}{D_{CPT}} < 0.083 \frac{q_c}{p_a}$ $q_b = q_{c,a}[0.5 - 0.25 \log_{10}(\frac{D}{D_{CPT}})]$ $Q_b = q_{c,a} \frac{\pi}{4}(D^2 - d^2)$	$\sigma'_r = 0.029 * q_c (\sigma_v'/p_a)^{0.13} (h/R^*)^{-0.38}$ $R^* = \sqrt{R^2 - r^2}$ $\Delta\sigma'_r = 2G \, \Delta r/R = 4G \, \Delta r/D$ $\eta = q_c (p_a \sigma'_v)^{-0.5}$ $G = q_c * 1/(0.0203 + 0.00125\eta - 1.216 * 10^{-6}\eta^2)$ $\sigma'_{r,total} = \Delta\sigma'_r + \sigma'_r$ $\tau_z = \sigma'_{r,total} \tan\delta_{cv}$
UWA-05	$A_{rb}{}^* = 1 - FFR(d/D)^2$ $q_b = q_{c,a}(0.15 + 0.45 A_{rb}{}^*)$	$\sigma'_r = 0.03 * q_c (A_{rs}{}^*)^{0.3} (h/D)^{-0.5}$ $A_{rs}{}^* = 1 - IFR_{average}(d/D)^2$ $G = 185 * q_c * \frac{(q_c/p_a)}{(\sigma'_v/p_a)^{0.5}})^{-0.75}$
HKU-12	$q_{annulus} = [1.063 - 0.045(L/D)] q_{c,a} \geq 0.46 \, q_{c,a}$ $q_{plug} = 1.063 e^{-1.933 PLR} q_{c,a}$ $Q_b = \frac{\pi}{4}[d^2 q_{plug} + (D^2 - d^2) q_{ann}]$	$Q_s = \pi D L \int_0^1 \tau_z d\xi$ $\rho = 1 - PLR(d/D)^2 > 0$ $\sigma'_r = 0.03 * q_c (\rho)^{0.3} (L/D)^{-0.5} (1 - \xi)^{-0.5} \leq 0.021 q_c (\rho)^{0.3}$ $D^* = (D^2 - PLR \, d^2)^{0.5}$ $\Delta\sigma'_r = 4G \, \Delta r/D^*$
Remarks	D_{CPT} is diameter of CPT equipment = 0.036m; Δ_r is assumed to be 0.00002m; p_a is atmospheric pressure at 100kPa; $\sigma'_{r,total}$ is the total radial stress and D_r was determined by the following correlation proposed by Jamiolkowaski et al. in 2003 $D_r = 100 * \frac{1}{3.1} \ln[\frac{q_c/p_a}{18(\sigma'_v/p_a)^{0.5}}]$	

4. Database

A database of 26 open-ended steel piles was compiled, summarising their configurations, settings, and references. It included 17 piles from Zhejiang University – Imperial College Database (ZJU-ICL Database) (Yang et al., 2015), 2 piles in Tokyo Bay (Kikuchi et al., 2007; Saitou et al., 2011), 3 piles from Korea (Ko & Jeong, 2015), 1 pile in Indiana, USA (Han et al., 2019), and 3 piles from China (Hu et al., 2020). Most data are CPT-based, except for the three Korean piles, which use SPT data. SPT-CPT correlation follows Robertson et al. (1983). The pile database is presented in Table 2 such that measured total capacity ranges from 1,246kN to 34,850kN.

Table 2. Database summary under this study.

#	Site name	Pile No.	Diameter (*mm*)	Wall Thickness (*mm*)	Pile Length L (*m*)	Measured Total Capacity (*kN*)	Measured Base Capacity (*kN*)	Measured Shaft Capacity (*kN*)	Settlement at measured capacity (*mm*)	Reference
1	Drammen	16-P1-11	813	12.5	11	1210	-	-	81.3	Yang et al. (2015) with original references stated
2	Drammen	25-P2-15	813	12.5	15	1890	-	-	NA	
3	Drammen	25-P2-25	813	12.5	25	2700	-	-	NA	
4	Dunkirk	C1-C	457	13.5	10	2820	-	-	32.5	
5	Euripides	Ia	763	35.6	30.5	7400	4000	3400	76.3	
6	Euripides	Ib	763	35.6	38.7	13000	3500	9500	76.3	
7	Euripides	Ic	763	35.6	47	18800	4750	14050	76.3	
8	Euripides	II	763	35.6	46.7	18400	4570	13830	76.3	
9	Hoogzand	1-C	356	16	7	2440	1310	1130	35.6	
10	Hoogzand	3-C	356	20	5.3	1950	-	-	35.6	
11	Hound Point	P(O)-C	1220	24.2	26	7000	3000	4000	122	
12	Mobile Bay	AL 1	324	25.4	15.2	1246	-	-	24	
13	Mobile Bay	AL 2	324	25.4	42.7	3350	-	-	32.4	
14	Pigeon River	P2	356	32	7	1275	909	366	35.6	
15	Shanghai	ST-1	914	20	79	15560	4100	11460	91.4	
16	Shanghai	ST-2	914	20	79.1	17080	2510	14570	91.4	
17	Tokyo Bay (ZJU-ICL)	TP	2000	34	30.6	34680	8742	25938	200	
18	Tokyo Bay (Kikuchi)	TP4	1500	28	73.5	22400	15700	6700	75	Kikuchi et al. (2007); Saitou et al. (2011)
19	Tokyo Bay (Kikuchi)	TP5	1500	28	86	18300	11300	7000	30	
20	Korea	TP-1	508	50.8	8.6	1031	320	711	50	Ko and Seong (2015)
21	Korea	TP-2	711.2	50.8	11.4	2240	660	1580	20	
22	Korea	TP-3	914.8	50.8	15.5	3100	951	2149	35	
23	Wabash River	OEP	660	50.5	30.48	4782	2220	2562	66	Han et al. (2019)
24	China A	S1	2000	28	55	32800	17607	15193	55	Hu et al. (2020)
25	China A	S2	2000	28	53	34850	17958	16892	55	
26	China B	S3	1800	30	29.3	12650	5650	7000	40	

The distribution of the selected pile tests in terms of pile length *L* and pile diameter *D* is presented in Figure 2a to 2b.

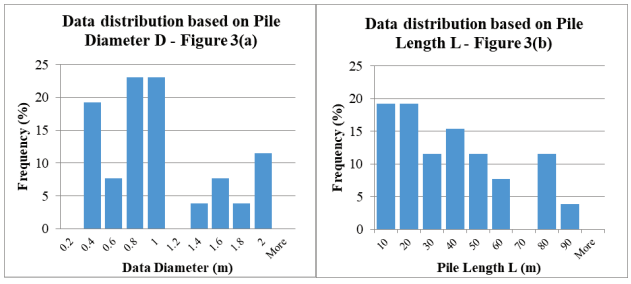

Figure 2. Database distribution: (a) against pile diameter; and (b) against pile length.

5. Results of analytical methods

Table 3 summarises the prediction with standard deviation (SD) and coefficient of variance (COV).

Table 3. Results of estimation of axial capacity.

$Q_{total}/Q_{measured}$					
Method	**API**	**GEO**	**ICP-05**	**UWA-05**	**HKU-12**
Mean	1.150	1.090	0.820	0.900	0.910
SD	0.741	0.784	0.351	0.316	0.311
COV	0.644	0.719	0.428	0.351	0.342
$Q_b/Q_{measured}$					
Mean	1.630	0.260	0.780	1.180	1.070
SD	1.188	0.195	0.407	0.523	0.439
COV	0.729	0.748	0.522	0.443	0.410
$Q_s/Q_{measured}$					
Mean	0.700	1.600	0.980	0.870	0.900
SD	0.359	1.109	0.515	0.472	0.471
COV	0.513	0.693	0.525	0.543	0.523

In general, CPT-based methods consistently outperform technical standards. HKU-12 provides the most accurate predictions in nearly all categories except variance of base capacity, followed by UWA-05. CPT-based methods yield a slightly conservative axial capacity, making them economical in practice. Unlike the empirical and dimensionless coefficients in technical standards, CPT-based methods rely on laboratory-based or CPT-correlated parameters. HKU-12 further enhanced the measurement of plug length from FFR to PLR to enable the single measurement of plug extent upon installation, on actual site work.

In contrast, technical standards exhibit significantly greater variability, with nearly doubled SD and COV. Over-prediction is likely due to the reliance on Nq and β without sufficient parameters to represent pile behaviours. Despite having comparable prediction performance in total capacity, API and GEO work differently in base capacity and shaft capacity predictions. API (2007) does not consider partial plugging, despite its importance in base resistance. GEO (2006) limits the base pressure at 5MPa with a safety factor of 2.5 for the entire pile tip area, with an additional Factor of Safety of 0.5 applied. These greatly constrain the estimated base capacity.

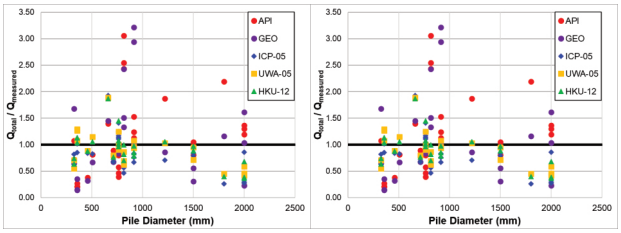

Figure 3. Relations of predicted total capacity and pile diameter (left) and pile length (right).

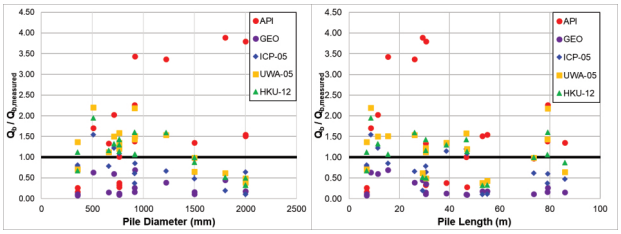

Figure 4. Relations of predicted base capacity with pile diameter (left) and pile length (right).

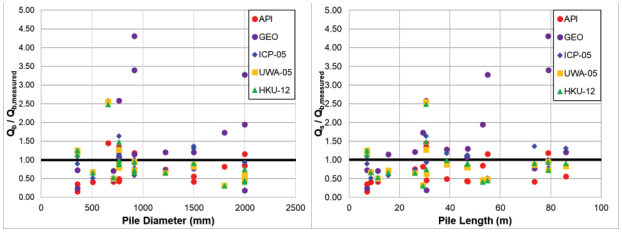

Figure 5. Relations of predicted shaft capacity with pile diameter (left) and pile length (right).

This study adopted the shaft resistance coefficient from Table 6.3 in GEO Publication No. 1/2006. The wide range of recommended values may lead to an overestimation of shaft capacity, possibly due to the absence of a limiting value. While GEO currently caps shaft resistance at 150 *kPa* for bored piles in granular soils (Section 6.4.4.3), a similar limit for steel pipe piles could be proposed when more load-test data become available. This highlights that the method requires careful justification of its coefficients, unlike CPT-based approaches where parameters are directly obtained from tests and correlations.

In recent years, open-ended steel pipe piles have been successfully installed in the waters of Hong Kong. Shea et al. (2022) presented testing results from the Offshore LNG Terminal. However, there is a lack of static load test data for evaluating the pile capacity. Shea et al. suggested the high Factor of Safety (FOS) in the local code of practice makes the test infeasible offshore. This highlights the limitation that the local industry lacks data to support the use of CPT-based methods in the territory.

6. FEM Model

6.1. Setup

In this study, PLAXIS 3D (Version 20) was used to model an open-ended steel pipe pile. The model featured a 10-node mono-pile using plate elements. Boundary conditions were set at one pile length from the centre, while the z-direction model extent (L+6D) followed the maximum influence zone proposed by Yang (2004). The hardening soil model was selected to simulate stiffness variations during the loading phase (PLAXIS, 2019).

The pile was modelled as a circular steel plate containing soil clusters within its hollow section. Interfaces were extended 1m beyond the pile tip to minimise modelling errors, while the Rinterface feature was used to represent soil–pile interactions. Plugging effects were simulated in later stages through selective soil removal inside the pile. A snapshot of the PLAXIS 3D model is presented in Figure 6.

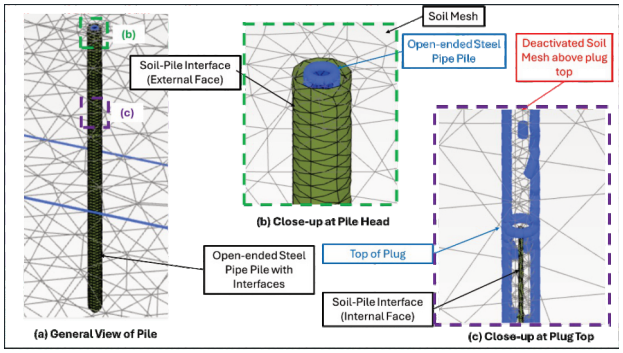

Figure 6. PLAXIS model setup.

6.2. Application for FEM modelling

In this study, three piles are chosen for FEM modelling, including Pile No. 12 in Mobile Bay, US, Pile No. 17 in Tokyo Bay, and Pile No. 21 in Korea. CPT profiles, if any, and Geological Profile are presented in Figure 7 below.

(a)

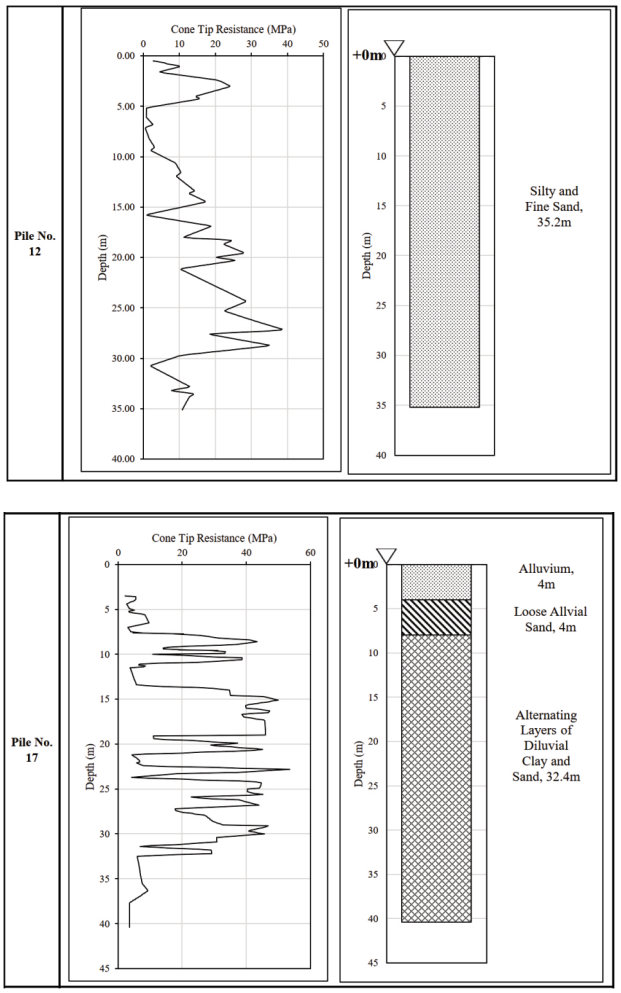

Figure 7. (a) Geological information of Pile Nos. 12 and 17; and (b) Geological information of Pile No. 21.

6.3. Pile modelling details

Two types of loading are applied to the structure in the simulation. The first is vertical loading at the pile top, where the pile's settlement was prescribed in the model, allowing the computation of corresponding loading. The second type of loading simulates the effect of installation. Based on the FEM model by Dijkstra et al. (2006), for a concrete displacement pile, a horizontal displacement equal to 7.5% of the pile radius was applied along the shaft, while a vertical displacement of 7.5 times the pile radius was applied at the pile tip.

The simulation consisted of four stages:

I. Initial Stage: Simulated in-situ soil response.

II. Installation Effect Stage: Applied displacements as per Dijkstra et al. (2006) to simulate soil deformation.

III. Pile Installation Stage: Activated the pile cluster

IV. Loading Stage: Applied load to generate a load–settlement curve

Table 4 summarises the input items for the FEM model.

Table 4. Input for the FEM model.

Parameter	Pile No. 12	Pile No. 17	Pile No. 21
Pile Name	AL1	TP	TP-2
Location	Mobile Bay, USA	Tokyo Bay, Japan	Korea
Pile Diameter (*mm*)	324	2000	711.2
Wall Thickness (*mm*)	25.4	34	50.8
Pile Length (*m*)	15.2	30.6	11.4
Plug Length (*m*)	12.5	30.6	8.66
Unit Weight (kN/m^3)	Silty and Fine Sand: 19	Alluvium: 19 Loose Alluvial Sand: 19 Alternating Layers of Diluvial Clay and Sand: 17.77	Reclaimed Fill: 17.6 Sand: 18
Soil Stiffness (*MPa*)	Silty and Fine Sand: 42	Alluvium: 12 Loose Alluvial Sand: 19 Alternating Layers of Diluvial Clay and Sand: 33	Reclaimed Fill: 13 Sand: 15
Poisson's Ratio	Silty and Fine Sand: 0.2	Alluvium: 0.2 Loose Alluvial Sand: 0.23 Alternating Layers of Diluvial Clay and Sand: 0.23	Reclaimed Fill: 0.3 Sand: 0.3
Friction Angle (°)	Silty and Fine Sand: 38	Alluvium: 42 Loose Alluvial Sand: 40 Alternating Layers of Diluvial Clay and Sand: 40	Reclaimed Fill: 32 Sand: 33

6.4. Modelling results

The piles were modelled under various combinations of prescribed displacements. The displacement combinations and respective results in the form of load–settlement curves are shown in Figure 8 below.

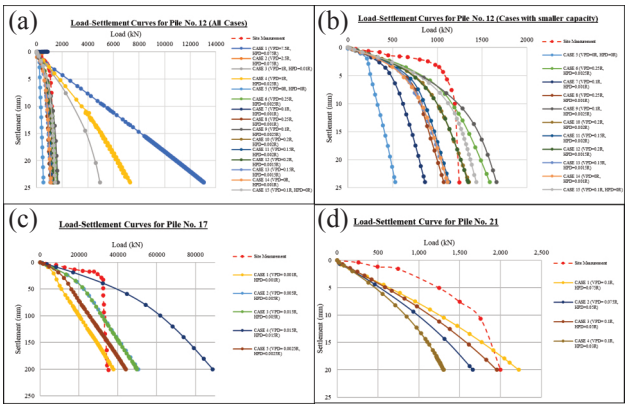

Note: HPD: Horizontal Prescribed Displacement; VPD: Vertical Prescribed Displacement

Figure 8. Load–settlement curves (Pile No. 12) (a) for all cases; (b) for cases of smaller loadings; (c) Load–settlement curves (Pile No. 17) ; and (d) Load–settlement curves (Pile No. 21).

From the results of Pile No. 12, it was found that Dijkstra's original prescribed displacements—7.5%R horizontally and 7.5R vertically—were excessive for open-ended steel pipe piles. These values were developed for concrete displacement piles, which differ in base contact area and overall stiffness. The analyses showed that much smaller displacements yielded significantly better agreement with field results.

Table 5 summarises the relation between the best estimation of prescribed displacements and pile parameters.

Table 5. Best-fit prescribed displacement and pile configurations.

Parameter	**Pile No. 12 (AL1)**	**Pile No. 17 (TP)**	**Pile No. 21 (TP-2)**
Location	Mobile Bay, USA	Tokyo Bay, Japan	Korea
Pile Diameter, D (*mm*)	324	2000	711.2
Radius, R (*mm*)	162.0	1000.0	355.6
Wall Thickness (*mm*)	25.4	34	50.8
Pile Length (*m*)	15.2	30.6	11.4
Plug Length (*m*)	12.5	30.6	8.66
Best-Fit Vertical Displacement (V)	24.30 mm **(15%R)**	1.00 mm **(0.1%R)**	35.56 mm **(10%R)**
Best-Fit Horizontal Displacement (H)	0.32 mm **(0.2%R)**	1.00 mm **(0.1%R)**	17.78 mm **(5%R)**

The following findings were found:

• Influence of plugging on prescribed displacements

Fully coring piles (e.g., Pile No. 17) required very small best-fit prescribed displacements (≈0.1%R), whereas partially plugged piles (Pile No. 12 and Pile No. 21) required substantially larger values (often >5%). This indicates a strong link between the extent of soil plugging and the magnitude of installation-induced displacement required to replicate field behaviour.

• Effect of wall thickness

Pile No. 21 exhibited unusually large best-fit horizontal displacements. Its relatively thick steel wall relative to its length and diameter significantly increases the pile's structural stiffness, suggesting that greater lateral movement may occur during driving before sufficient soil–pile interaction develops.

• Sensitivity to horizontal displacement

Pile capacity was consistently more sensitive to horizontal than vertical prescribed displacement. For example, in Pile No. 17, tripling the vertical displacement produced negligible change in capacity (Cases 2 and 3), whereas tripling the horizontal displacement approximately doubled the capacity (Case 4). Similar patterns were observed in Pile No. 12 (Cases 7–9) and Pile No. 21 (Cases 1–2, 4), although the magnitude of sensitivity varied with pile size.

• Difference in curve shape from field measurements

The FEM load–settlement curves showed steady, continuous settlement with increasing load, differing from the site curves, which exhibited a clearer transition toward failure. This behaviour persisted even in cases without installation effects, suggesting that the discrepancy is largely attributable to soil parameters that were correlated or assumed, rather than the installation modelling itself.

Overall, while the FEM model successfully simulated axial behaviour trends for open-ended steel pipe piles, further refinement is required. In particular, more detailed modelling of soil–pile interface stresses and improved calibration of horizontal installation displacements are recommended, as installation effects are unlikely to be uniform along the pile length and are dynamic effects.

7. Comparison of analytical and FEM method

FEM methods and analytical methods offer distinct advantages.

FEM models simulate pile behavior comprehensively. In this study, PLAXIS 3D was used to evaluate axial capacity and generate load–settlement curves, but the numerical environment also enables deeper investigation of soil–pile mechanisms—for example, examining interface behaviour, stress profiles, and load transfer to infer shaft resistance. With further development, FEM can also be extended to study lateral capacity and more complex loading scenarios.

FEM models surpass analytical methods in variability and flexibility. Analytical methods are empirical and rely on simplifying assumptions, which can restrict their accuracy across diverse geological settings. Jardine et al. (2005) recorded that ICP-05 tends to predict pile capacity at 100 days after installation, while test data typically rely on settlements of 10% of the pile diameter, giving rise to differences in estimation. On the contrary, multiple construction and loading stages can be modelled with settlement and loading responses to be retrieved directly from numerical output.

However, analytical methods offer practicality. They generally require fewer inputs, relying mainly on commonly available soil parameters and pile geometry. FEM, by comparison, demands advanced constitutive parameters, careful mesh design, and detailed modelling decisions, all of which increase effort and computational cost. Under constraints of budget, time, or available soil data, analytical methods remain valuable design tools that can provide quick and suitably conservative estimates when applied correctly.

8. Conclusion

This study compared five analytical methods for estimating the capacity of open-ended steel pipe piles in sand. The results show that CPT-based methods outperform technical standards and therefore offer a cost-effective design basis. Among them, HKU-12 gave the closest but still conservative predictions. Furthermore, this study portrays FEM models to simulate axial capacity in PLAXIS 3D. To further improve design reliability, instrumented static load tests are recommended for future calibration and verification.

Notes on contributors

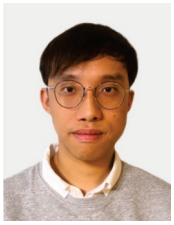

Ir Harry Ho Kan Lee received his BEng (Civil Engineering) with First Class Honours and M.Sc. (Geotechnical Engineering) from the University of Hong Kong in 2017 and 2022, respectively. He joined the Geotechnical Business Line of AECOM Asia Company Limited in 2017. He has been a member of HKIE since 2023 and is now working as a Project Engineer focusing on tunnel projects.

Ir Prof Jun Yang joined the faculty of the University of Hong Kong in 2003 and is currently a full professor at the Department of Civil Engineering. His expertise is geotechnical engineering, offshore geotechnics, and geomechanics. He has published widely in leading journals in his fields and has been listed by Clarivate among the world's top 1% scholars by citations. He is a Fellow of HKIE, ICE, and ASCE.

References

[1] American Petroleum Institute (2007). *Recommended practice for planning, designing and constructing fixed offshore platforms – working stress design.* USA: American Petroleum Institute.

[2] Dijkstra J, Broere W and van Tol A F (2006). *Numerical investigation into stress and strain development around a displacement pile in sand.* Proceedings of the sixth European Conference on Numerical Methods in Geotechnical Engineering, pp. 595-600.

[3] Geotechnical Engineering Office (2006). *GEO Publication No. 1/2006 - Foundation Design and Construction*. Hong Kong: HKSAR Government.

[4] Han F, Ganju E, Prezzi M, Salgado R and Zaheer M (2020). Axial Resistance of open-ended pipe pile driven in gravelly sand. Géotechnique, 70(2), pp. 138-152

[5] Hu Z, Huang S, Liu W and Si J (2020). Study on Shaft Friction of Open-ended Steel Pipe Piles for Offshore Wind Farms Based on Field Tests, J. Geotech. Eng., 15(1), pp. 47-54.

[6] Jamiokowski M, Lo Presti D C F and Manassero M (2003). Evaluation of Relative Density and Shear Strength of Sands from CPT and DMT. ASCE Geotechnical Special Publication, 119, pp. 201–238.

[7] Jardine R J, Chow F, Overy R and Strading J R (2005). *ICP design methods for driven piles in sands and clays*. London: Thomas Telford.

[8] Kikuchi Y, Mizutani M and Yamashita H (2007). *Vertical bearing capacity of large diameter steel pipe piles*. In: Proceedings of Advances in Deep Foundations. London: Taylor and Francis, pp. 177-182.

[9] Ko J and Jeong S (2015). Plugging effect of open-ended piles in sandy soil. *Can. Geotech. J.*, 52(5), pp. 535-547.

[10] Ko J, Jeong S and Lee J K (2015). Large deformation FE analysis of driven steel pipe piles with soil plugging. *Computers Geotechnics.*, 71, pp. 82-97

[11] Lehane B M and Randolph M F (2002). Estimation of a minimum base resistance for driven pipe piles in siliceous sand. *J. Geotech. Geoenviron. Eng., ASCE*, 128(3), pp. 198-205.

[12] Lehane B M, Schneider J A and Xu X (2005a). *CPT based design of driven piles in sand for offshore structures*. Perth: University of Western Australia.

[13] Lehane B M, Schneider, J A and Xu X (2005b). *A review of design methods for offshore driven piles in siliceous sand*. Perth: University of Western Australia.

[14] Paik K and Salgado R (2003). Determination of bearing capacity of open-ended piles in sand. *J. Geotech. Geoenviron. Eng*, 129(1), pp. 46-57.

[15] Paik K H and Lee D R (1993). Behavior of soil plugs in open ended model piles driven into sands. *Marine Georesources Geotechnlogy*, 11(4), pp. 353-373.

[16] Paikowsky S G, Whitman R V and Baligh M M (1989) A new look at the phenomenon of offshore pile plugging. *Marine Geotechnology*, 8(3), pp. 213-230.

[17] PLAXIS (2019). *PLAXIS CONNECT Edition V20 Manual*. The Netherlands: Plaxis bv, Bentley Systems

[18] Robertson P K and Campanella R G (1983). Interpretation of cone penetration tests: Part I: Sand. *Can. Geotech. J.*, 20, pp. 718-733

[19] Robertson P K, Campanella R G and Wightman A (1983). SPT-CPT Correlation. *J. Geotech. Eng.*, 109(11), pp. 1449-1459.

[20] Saitou Y, Kikuchi Y, Kusakabe O, Kiyomiya O, Yoneyama H and Kawakami T (2011). Application of steel pipe pile loading tests to design verification of foundation of the Tokyo Gate Bridge. *J. Society of Civil Engineers, Ser. C (Geosphere Engineering)*, 67(4), pp. 544-557 (In Japanese)

[21] Shea V, Li D, Shum D and Chu F (2022) Large diameter open-end steel piled foundations for the Hong Kong offshore LNG terminal – design and installation. *Proc. of The HKIE Geotechnical Division 42nd Annual Seminar: A New Era of Metropolis and Infrastructure Developments in Hong Kong, Challenges and Opportunities to Geotechnical Engineering*, pp. 174-186.

[22] Vesic A S (1970). Tests on instrumented piles, Ogeechee River Site. *J. Soil Mechanics and Foundations Division*, ASCE, 96(2), pp. 561-584

[23] Yang J (2006). Influence Zone for End-Bearing of Piles in Sand. *J. Geotech. Geoenviron. Eng, ASCE*, 132(9), pp. 1229-1237.

[24] Yang Z, Jardine R, Guo W and Chow F (2015). A new and openly accessible database of tests on piles driven in sands. *Géotechnique Letters*, 5(1), pp. 12-20

[25] Yu F and Yang J (2012a). Base capacity of open-ended Steel Pipe Piles in Sand. *J. Geotech. Geoenviron. Eng, ASCE*, 138, pp. 1116-1128

[26] Yu F and Yang J (2012b). Improved evaluation of interface friction of steel pipe pile in sand. *J. Performance Constructed Facilities, ASCE*, 26, pp. 170-179.